

Efficient numerical solution of the time - dependent Schrödinger equation for deep tunneling

Nicolae Carjan^a , Margarit Rizea^b , Dan Strottman^c

^a Centre d'Etudes Nucleaires de Bordeaux - Gradignan,
BP 120 Le Haut Vigneau, 33175 Gradignan Cedex, France

E-mail: carjan@in2p3.fr

^b National Institute of Physics and Nuclear Engineering

"Horia Hulubei"

P.O. Box MG-6, Bucharest, Romania

E-mail: rizea@theor1.theory.nipne.ro

^c Theoretical Division, Los Alamos National Laboratory,

Los Alamos, NM 87544, USA

E-mail: dds@lanl.gov

Abstract

The numerical challenge associated with the time-dependent approach to the general problem of the decay of a metastable state by quantum - tunneling is discussed and methods towards its application to concrete problems are presented. In particular, different artificial boundary conditions were implemented in order to reduce the reflections of the wave packet at the numerical boundaries. They are illustrated and optimized for the deep - tunneling case of ground - state proton decay.

Keywords: time dependent Schrödinger equation; Crank - Nicolson, multiple step differencing, Chebyshev methods; transparent, absorbing, discrete transparent boundary conditions; deep tunneling; decay rate.

1 Introduction

The problem of the decay of metastable states is of major importance for the understanding of many physical, chemical or biological processes. A metastable state, or a quasi-stationary state, is defined as a state of local stability which decays with a finite lifetime towards a true stable minimum. When the temperature of the decaying system is low, quantum tunneling is the dominant decay process. An intuitive and precise approach to this phenomenon involves the numerical solution of the time-dependent Schrödinger equation, TDSE ([1] - [3]). Contrary to the stationary approximations (WKB and DWBA) that have been widely used in the past, this new approach is exact to the numerical accuracy and can therefore be used to test their validity. In certain cases, however, this approach poses a complicated numerical problem.

The different methods that have been developed for solving numerically the TDSE consist of a discretization both in space and time. To obtain a realistic representation of the problem to be solved, the mesh size Δx and the time step Δt have to be, respectively, much smaller than the spatial dimension and the time scale of a particular problem. Consequently, we are often faced with a difficult numerical task : computers with high speed and large memory are needed.

When a metastable state decays into continuum (as in alpha decay, nuclear fission, etc) the physical domain extends to plus infinity. Since we can handle numerically only a finite portion of it, and to avoid unwanted interference, we must impose artificial boundary conditions that efficiently reduce the reflections on the numerical boundary.

In the experimentally accessible cases of relatively long - lived isomers (microseconds or more), there is an additional difficulty : double or even quadruple precision is necessary to calculate extremely small increases $\Delta\rho$ of the tunneling probability during each time step Δt . One has also to prepare carefully the initial wave packet in order to diminish drastically the contributions of the high - energy components which have much higher tunneling probabilities and cover the signal we are looking for.

It is therefore necessary to systematically investigate these difficulties of calculating on large grids, for long times, small decay rates in order to develop methods to overcome them. For deep tunneling case they are present even in the one - dimensional case.

The aim of the present work is to find which combination of artificial boundary condition and numerical scheme for TDSE is most efficient from a computational point of view. Although it uses for simplicity the one-dimensional TDSE, it was done having in mind the subsequent generalization to the more prestigious two dimensional case.

In the next section the most relevant numerical schemes will be briefly reviewed emphasizing their main features. In the third section the artificial boundary conditions will be illustrated through three methods : the **transparent** boundary conditions [11], [12], the **absorbing** boundary conditions [15], and the **discrete transparent** boundary conditions [20].

In the fourth section these methods have been implemented for the first time in the difficult case of deep quantum tunneling and optimized to reduce the spatial grid to a manageable size.

In particular the performances of different combinations of artificial boundary conditions and numerical schemes have been compared. Two low lying metastable states in spherical ^{109}I nucleus have been chosen for this purpose. The characteristics of one of these states ($Q_p = 0.829$ MeV, $L = 2$) correspond to the ground - state proton decay experimentally observed in this nucleus ($t_{1/2} = 8.82\mu$ s). The other state ($Q_p = 0.711$ MeV, $L = 4$) was selected to show the ability of the present approach to describe isomers with even longer lifetime (0.215 s).

2 Numerical procedures for solving TDSE

Let us consider the one dimensional TDSE , with a time - independent potential $V(x)$:

$$i\hbar\frac{\partial\psi(x,t)}{\partial t} = H\psi(x,t), \quad x \in \mathbf{R}, t > 0, \quad (2.1)$$

where

$$H = \frac{-\hbar^2}{2m}\frac{\partial^2}{\partial x^2} + V(x). \quad (2.2)$$

By supposing that

$$\psi(x,0) = \psi^I(x), \quad \psi^I \in L^2(\mathbf{R}),$$

we search for a solution $\psi(x,t) \in L^2(\mathbf{R})$ for any $t > 0$.

The formal solution of (2.1) can be expressed by:

$$\psi(t + \Delta t) = \exp\left(\frac{-iH\Delta t}{\hbar}\right)\psi(t). \quad (2.3)$$

Various schemes have been proposed to approximate the exponential function. We cite Crank-Nicolson (CN), multi-step differencing (MSD), Chebyshev, "leap - frog", split operator and short iterative Lanczos propagation (see, e.g., [4] - [9]). We shall focus on the first three methods, whose main features will be described in the next subsections.

2.1 Crank - Nicolson method

In this scheme the exponential is approximated by the Cayley transform (i.e., a rational approximation by two polynomials of degree 1) ([4], [5]):

$$\psi(t + \Delta t) = \frac{1 - iH\Delta t/2\hbar}{1 + iH\Delta t/2\hbar}\psi(t) + O((H\Delta t)^3). \quad (2.4)$$

The spatial interval $[x_{min}, x_{max}]$ is divided in equidistant points with a mesh Δx , resulting the grid $x_{min} = x_1, x_2, \dots, x_M = x_{max}$. We denote by ψ_j^n the solution at the time n and the point x_j . In calculating $H\psi_j^n$ an approximation of the second derivative is needed. In the CN scheme, this is done by the finite difference formula:

$$\frac{\partial^2 \psi_j^n}{\partial x^2} \approx \frac{\psi_{j+1}^n - 2\psi_j^n + \psi_{j-1}^n}{\Delta x^2}. \quad (2.5)$$

According to (2.4), we can write:

$$(1 + iH\Delta t/2\hbar)\psi_j^{n+1} = (1 - iH\Delta t/2\hbar)\psi_j^n. \quad (2.6)$$

By using the approximation (2.5) and noting $V_j = V(x_j)$, the following system results for determining the values ψ_j^{n+1} :

$$\psi_{j+1}^{n+1} + (\lambda - \mu V_j - 2)\psi_j^{n+1} + \psi_{j-1}^{n+1} = -\psi_{j+1}^n + (\lambda + \mu V_j + 2)\psi_j^n - \psi_{j-1}^n, j = 1, 2, \dots, M \quad (2.7)$$

where

$$\lambda = \frac{4im\Delta x^2}{\hbar\Delta t}, \quad \mu = \frac{2m\Delta x^2}{\hbar^2}. \quad (2.8)$$

The linear system (2.7) is tridiagonal and can be solved fast and accurately by a special adapted procedure (see [5], chapter 2).

This scheme is unitary and conserves the norm. (see, e.g., [6]).

In order to study the stability of the scheme we use the Courant - Lewy - Friedrichs criterion (see, e.g. [5]), considering the error in ψ_j^n of the form

$$\epsilon_j^n = \hat{\epsilon}^n \exp(iqx_j) \quad (2.9)$$

where q is a real spatial wave number, which can have any value.

Thus, the error is split into a part depending on time and another depending on space. We try to see the evolution of this error, by considering also the error ϵ_j^{n+1} in ψ_j^{n+1} .

The exact solutions at times n and $n + 1$ will be $\Psi_j^n = \psi_j^n + \epsilon_j^n$ and $\Psi_j^{n+1} = \psi_j^{n+1} + \epsilon_j^{n+1}$.

We introduce them into the relation:

$$(1 + iH\Delta t/2\hbar)\Psi_j^{n+1} = (1 - iH\Delta t/2\hbar)\Psi_j^n, \quad (2.10)$$

corresponding to Crank-Nicolson scheme.

By considering the approximation of the hamiltonian

$$H\Psi_j \approx \frac{-\hbar^2}{2m} \frac{\Psi_{j+1} - 2\Psi_j + \Psi_{j-1}}{\Delta x^2} + V_j \quad (2.11)$$

one obtains:

$$\{1 + i[\alpha(2\cos(q\Delta x) - 2) + \frac{\Delta t}{2\hbar}V_j]\}\hat{\epsilon}^{n+1} = \{1 - i[\alpha(2\cos(q\Delta x) - 2) + \frac{\Delta t}{2\hbar}V_j]\}\hat{\epsilon}^n \quad (2.12)$$

where

$$\alpha = -\frac{\hbar^2 \Delta t}{2m} \frac{1}{2\hbar \Delta x^2}.$$

The ratio $\hat{\epsilon}^{n+1}/\hat{\epsilon}^n$ is called the growth factor g . The stability is ensured if $|g|$ is not > 1 (otherwise the errors will grow exponentially).

From the above relation we get:

$$g = \frac{1 - i[\alpha(2\cos(q\Delta x) - 2) + \frac{\Delta t}{2\hbar}V_j]}{1 + i[\alpha(2\cos(q\Delta x) - 2) + \frac{\Delta t}{2\hbar}V_j]} \quad (2.13)$$

and thus $|g| = 1$.

This shows that CN scheme is unconditionally stable.

2.2 Multiple step differencing methods

The multiple step differencing schemes are explicit methods, thus avoiding a linear system solution as is the case with CN method, which is implicit. However, they are only conditionally stable, which imposes restrictions on the time step. The simplest is the second order differencing scheme - MSD2 (see [6], [9]), which is obtained by using the relation (2.3) for $t + \Delta t$ and $t - \Delta t$ and the expansion of the two exponentials in Taylor series, as follows:

$$\begin{aligned} \psi(t + \Delta t) - \psi(t - \Delta t) &= [\exp(-iH\Delta t/\hbar) - \exp(+iH\Delta t/\hbar)]\psi(t) = \\ &= -2iH\Delta t/\hbar\psi(t) + O((H\Delta t)^3). \end{aligned} \quad (2.14)$$

To obtain this formula, the Taylor series are truncated after the first 3 terms. Thus, in MSD2 the solution at time $n + 1$ is obtained from solutions at times n and $n - 1$ by the relation:

$$\psi^{n+1} = -\frac{2i\Delta t}{\hbar}H\psi^n + \psi^{n-1}. \quad (2.15)$$

Like in CN scheme, a spatial grid and a finite difference approximation of the second derivative is considered, leading to the following computational formula

$$\psi_j^{n+1} = -\frac{2i\Delta t}{\hbar} \left(-\frac{\hbar^2}{2m} \frac{\psi_{j+1}^n - 2\psi_j^n + \psi_{j-1}^n}{\Delta x^2} + V_j \right) + \psi_j^{n-1}. \quad (2.16)$$

The scheme is conditionally stable. In order to see this, we shall use again the Courant - Lewy - Friedrichs criterion. By considering the error in ψ_j^n of the form (2.9) and introducing the solutions in eq. (2.16), we obtain for the growth factor

$$g = \hat{\epsilon}^{n+1}/\hat{\epsilon}^n = \hat{\epsilon}^n/\hat{\epsilon}^{n-1} \quad (2.17)$$

the following equation :

$$g^2 + 2i\alpha_j g - 1 = 0 \quad (2.18)$$

where

$$\alpha_j = \frac{\Delta t}{\hbar} \left[-\frac{\hbar^2}{2m} \frac{2\cos(q\Delta x) - 2}{\Delta x^2} + V_j \right] \quad (2.19)$$

The solutions of equation (2.18) are :

$$g_{1,2} = -i\alpha_j \pm \sqrt{1 - \alpha_j^2} \quad (2.20)$$

If the condition $\alpha_j \leq 1$ is fulfilled, then

$$|g_1| = |g_2| = 1, \quad (2.21)$$

which shows that MSD2 is conditionally stable.

By taking $\alpha = \max_j \{\alpha_j\}$, the stability is ensured for all grid points if $\alpha \leq 1$. In fact, this condition leads to a relation between Δx and Δt , imposing restrictions on the space and time steps which can be used.

Higher order differencing schemes can also be obtained. In [10] differencing schemes of orders 4 and 6 are introduced.

The schemes MSD4 and MSD6 are more accurate than MSD2 with respect to Δt , but the conditions of stability are also more restrictive, requiring smaller time steps. There is a trade-off between the higher order accuracy and the condition of the stability.

We have to note that unlike the CN scheme, which requires only the usual initial wave function (at $t = 0$), to start MSD schemes we need also auxiliary initial wave functions at $t = \Delta t, 2\Delta t, \dots$. These can be prepared by using the Taylor expansion of the time evolution operator

$$\psi(t) = \exp\left(\frac{-iHt}{\hbar}\right)\psi(0) \approx \sum_{n=0}^{N_{order}} \frac{(-iHt/\hbar)^n}{n!} \psi(0) \quad (2.22)$$

where N_{order} is the order of MSD.

2.3 Chebyshev method

In this method the exponential operator is approximated by a polynomial expansion (see [7], [9]) :

$$\exp\left(\frac{-iH\Delta t}{\hbar}\right) \approx \sum_{n=0}^{N_b} a_n P_n\left(\frac{-iH\Delta t}{\hbar}\right). \quad (2.23)$$

The Chebyshev scheme approaches this problem in analogy to the approximation of a scalar function. Consider a scalar function $F(x)$ in the interval $[-1, 1]$. In this case it is known that the Chebyshev polynomial approximations are optimal, ensuring a minimal error in comparison with all polynomial approximations.

In the approximation of the evolution operator, the complex Chebyshev polynomials $\Phi_n(X)$ are used, replacing the scalar function by a function of an operator. In making this change, one has to examine the domain of the operator and adjust it to the range of definition of the Chebyshev polynomials. The range of definition of these polynomials is from $-i$ to i . This means that the Hamiltonian operator has to be renormalized by dividing it by $\Delta E_{grid} = E_{max} - E_{min}$, where $E_{min} = V_{min}$ and $E_{max} = V_{max} + K_{max}$ with $K_{max} = \sum_i \frac{\pi^2 \hbar^2}{2\mu \Delta x_i^2}$ where Δx_i is the grid spacing on the i 'th coordinate.

Also, for maximum efficiency, the range of eigenvalues is positioned from -1 to 1 by shifting the Hamiltonian to

$$H_{norm} = 2 \frac{H - I(\Delta E_{grid}/2 + E_{min})}{\Delta E_{grid}}. \quad (2.24)$$

Denoting $\alpha = \Delta E_{grid} t / 2\hbar$, the evolution of the wavefunction ψ can be approximated as

$$\psi(t) = e^{-(i/\hbar)(\Delta E_{grid}/2 + E_{min})t} \sum_0^{N_b} a_n(\alpha) \Phi_n(-iH_{norm}) \psi(0). \quad (2.25)$$

The first term on the right-hand side is a phase shift compensating the shift in the energy scale. The expansion coefficients become:

$$a_n(\alpha) = 2J_n(\alpha) \quad (2.26)$$

with $a_0(\alpha) = J_0(\alpha)$. J_n are the Bessel functions.

The use of eq. (2.25) requires the calculation of the operation of $\Phi_n(-iH_{norm})$ on $\psi(0)$. This is accompanied by the recursion relation of the Chebyshev polynomials

$$\phi_{n+1} = -2iH_{norm}\phi_n + \phi_{n-1} \quad (2.27)$$

with $\phi_n = \Phi_n(-iH_{norm})\psi(0)$.

The recurrence is started by $\phi_0 = \psi_0$ and $\phi_1 = -iH_{norm}\psi_0$.

The number of expansion terms needed to converge the sum in (2.25) is determined by the size of the time-energy phase space volume: $\alpha = \Delta E_{grid}t/2\hbar$. Examining the expansion coefficients as a function of n , one finds that when n becomes larger than α , the Bessel functions $J_n(\alpha)$ decay exponentially. This means that in a practical implementation, the maximum order N_b can be chosen such that the accuracy is dominated by the accuracy of the computer.

The efficiency of the Chebyshev scheme depends on ΔE_{grid} whose size determines the number of terms used in sum (2.25).

3 Artificial Boundary Conditions

The TDSE is a partial differential equation (of parabolic type) which is normally defined on an unbounded domain with definite boundary conditions (usually the solution should tend to zero towards the ends of the domain). In order to make this problem feasible for numerical treatment it is necessary to restrict the original problem to a finite interval. This approximation leads to reflections at the boundaries that affect the propagated wave function and to errors in the calculation of the physical quantities. One solution is to increase the spatial grid, but in many cases it is necessary to use very large intervals, which is costly in computer time and memory requirements. In order to eliminate or at least to reduce reflections, special procedures were conceived, thus allowing the use of smaller spatial computational domains. By these procedures special boundary conditions are imposed, which - obviously - should be consistent with the original boundary conditions on the entire space.

We shall present three kinds of such procedures, namely **Transparent Boundary Conditions** (TBC) [11],[12], **Absorbing Boundary Conditions** (ABC) [15] and **Discrete Transparent Boundary Conditions** (DTBC) [20]. They may be easily incorporated into the Crank-Nicolson scheme.

3.1 Transparent Boundary Conditions

Our TBC algorithm is based on some suggestions formulated by Hadley ([11], [12]) in a different context.

Let us consider the integral

$$\rho = \int_a^b |\psi|^2 dx \quad (3.1)$$

and calculate $\frac{\partial \rho}{\partial t}$ which is related to the energy conservation.

By simple manipulations, using TDSE eq.(2.1) we obtain:

$$\frac{\partial \rho}{\partial t} = \frac{i\hbar}{2m} [\psi^* \frac{\partial \psi}{\partial x} - \psi \frac{\partial \psi^*}{\partial x}]|_a^b = -F_b + F_a \quad (3.2)$$

where F_b represents the energy “flux” leaving the right boundary and F_a that entering through the left boundary. Since the treatment of the two boundaries is essentially identical, we will focus on the right boundary. We next make the important assumption that near this boundary

$\psi = \psi_0 \exp(ik_x x)$, where ψ_0 and k_x are complex constants, and k_x is (for the moment) unknown. With this assumption, F_b becomes

$$F_b = \frac{\hbar}{m} \text{Real}(k_x) |\psi(b)|^2. \quad (3.3)$$

Therefore, as long as the real part of k_x is positive, the contribution to the overall change in energy from this boundary will always be negative, i.e., radiative energy can only flow out of the problem region.

If we now consider the finite difference equivalent of (3.2) using the Crank-Nicolson scheme, it can be shown that the above energy balance relationship is preserved. Thus, assuming the same exponential dependence described above, we adjust the boundary value ψ_{M+1}^n (which without TBC is assumed to be 0) prior to the start of the $(n+1)$ th propagation step so that

$$\frac{\psi_{M+1}^n}{\psi_M^n} = \frac{\psi_M^n}{\psi_{M-1}^n} = \exp(ik_x \Delta x). \quad (3.4)$$

This determines k_x and the boundary condition for the new propagation step is thus

$$\psi_{M+1}^{n+1} = \psi_M^{n+1} \exp(ik_x \Delta x). \quad (3.5)$$

However, prior to the application of (3.5), the real part of k_x must be restricted to be positive to ensure only radiation outflow. In practice, this is done as follows. Let us note

$$\alpha = \exp(ik_x \Delta x) = \exp(i(k_1 + ik_2) \Delta x) = \exp(-k_2 \Delta x) \exp(ik_1 \Delta x).$$

We shall write:

$$\alpha = r + is = \rho \exp(i\theta) = \rho (\cos \theta + i \sin \theta).$$

Thus,

$$\rho = \exp(-k_2 \Delta x) = |\alpha|$$

and

$$\theta = \arctan(s/r) = k_1 \Delta x.$$

We want to keep $k_1 \geq 0$. As $k_1 < 0$ is equivalent to $\theta < 0$, we shall put in such a case $\theta = 0$.

Then we shall take $\alpha = \rho \exp(i\theta)$ with θ eventually set to 0 and the relation between ψ_{M+1} and ψ_M will be:

$$\psi_{M+1}^{n+1} = \alpha \psi_M^{n+1}. \quad (3.6)$$

The application of this condition implies a modification of the last equation (corresponding to $j = M$) of the system 2.7, which becomes:

$$(\alpha + \lambda - \mu V_M - 2) \psi_M^{n+1} + \psi_{M-1}^{n+1} = (-\alpha + \lambda + \mu V_j + 2) \psi_M^n - \psi_{M-1}^n \quad (3.7)$$

An important feature of the above procedure is that k_x is allowed to change as the problem progresses, thus eliminating the need for a problem-dependent adjustable parameter.

It should be mentioned that the stability criterion of Courant - Lewy - Friedrichs is also valid with this TBC introduced in Crank - Nicolson scheme, since the growth factor g has the form (2.13) for any index j (including $j = M$) even if the relation (3.6) is used in the last equation of Crank - Nicolson procedure.

With this procedure accurate values of the tunneling probability can be obtained with a much smaller spatial grid than is necessary without TBC procedure.

3.2 Absorbing Boundary Conditions

In this approach it is supposed that TDSE admits plane wave solutions of the form

$$\psi = e^{-i(\omega t - kx)}. \quad (3.8)$$

The idea is to construct an algebraic equation for k and ω and then to use the correspondence between the $x-t$ space and the $k-\omega$ space to construct a differential equation on the boundaries which is transparent for the plane waves.

By introducing the solution of form (3.8) into eq.(2.1) one obtains the relation

$$\hbar^2 k^2 = 2m(\hbar\omega - V). \quad (3.9)$$

This relation can be solved for k and yields

$$\hbar k = \pm \sqrt{2m(\hbar\omega - V)} \quad (3.10)$$

where the plus sign describes waves moving to the right boundary and the minus sign means waves moving to the left boundary. The left boundary has to be transparent for left-going waves and the right boundary must be transparent for right-going waves.

To transform (3.10) back into the $x-t$ space one needs an approximation for the square root which can be easily transformed into a differential equation at the boundary. Shibata ([13]) used a linear approximation of the square root function, while Kuska ([14]) used a rational function approximation.

Fevens and Jiang ([15]) have developed a more general approach to produce absorbing boundary conditions, which includes as special cases the previous methods. They have shown that the absorbing boundary conditions are equivalent to the following differential operator relation:

$$\Pi_{l=1}^p \left(i \frac{\partial}{\partial x} + \frac{ma_l}{\hbar} \right) \psi = 0. \quad (3.11)$$

where $a_l \in \mathbf{R}$ are wave velocities.

Between the $x-t$ space and $k-\omega$ space the following correspondence exists:

$$k \Leftrightarrow -i \frac{\partial}{\partial x}, \quad \omega \Leftrightarrow i \frac{\partial}{\partial t}. \quad (3.12)$$

Using it one arrives to differential equations to be satisfied at the boundary. The value of p represents the order of absorbing condition.

We will consider the case $p = 3$

Making use of the correspondence (3.12) we obtain the following equation from eq.(3.11)

$$\left(-k + \frac{ma_1}{\hbar}\right)\left(-k + \frac{ma_2}{\hbar}\right)\left(-k + \frac{ma_3}{\hbar}\right) = 0 \quad (3.13)$$

Using (3.10) to substitute for k^2 , this simplifies to the relation

$$\hbar k = \frac{2mh_1(\hbar\omega - V) + h_3}{2m(\hbar\omega - V) + h_2}, \quad (3.14)$$

where

$$\begin{aligned} h_1 &= m(a_1 + a_2 + a_3), \\ h_2 &= m^2(a_1a_2 + a_2a_3 + a_3a_1), \\ h_3 &= m^3a_1a_2a_3. \end{aligned}$$

From (3.14) we obtain the equation:

$$\hbar k\left(\frac{h_2}{2m} - V\right) + \hbar^2 \omega k - \hbar h_1 \omega - \left(\frac{h_3}{2m} - h_1 V\right) = 0. \tag{3.15}$$

Using again the correspondence (3.12) the following partial differential equation is obtained:

$$-i\hbar\left(\frac{h_2}{2m} - V\right)\psi_x + \hbar^2 \psi_{tx} - i\hbar h_1 \psi_t - \left(\frac{h_3}{2m} - h_1 V\right)\psi = 0. \tag{3.16}$$

Writing this equation for $x = x_j$ and $t = t_n$ and using for derivatives finite difference approximations we get the following absorbing boundary condition:

$$\begin{aligned} (\alpha - \beta - \gamma - \delta)\psi_{M-1}^{n+1} + (-\alpha + \beta - \gamma - \delta)\psi_M^{n+1} = \\ (-\alpha - \beta - \gamma + \delta)\psi_{M-1}^n + (\alpha + \beta - \gamma + \delta)\psi_M^n \end{aligned} \tag{3.17}$$

where

$$\begin{aligned} \alpha &= \frac{i\hbar}{2\Delta x} \left(\frac{h_2}{2m} - V_{M-1}\right), \quad \beta = \frac{\hbar^2}{\Delta t \Delta x}, \\ \gamma &= \frac{i\hbar h_1}{2\Delta t}, \quad \delta = \frac{1}{4} \left(\frac{h_3}{2m} - h_1 V_{M-1}\right). \end{aligned}$$

Eq.(3.17) replaces the last equation in linear system (2.7) derived from the Crank - Nicolson scheme.

Of course, the quality of the approximation increases with p.

3.3 Discrete Transparent Boundary Conditions

This procedure originates from an **analytic** TBC derived by several authors from various applications fields (see [16] - [19]).

The original *whole - space problem* is cut into three subproblems, the interior problem on the domain $0 < x < L$, and a left and right exterior problem. They are coupled by the assumption that ψ and ψ_x are continuous across the artificial boundaries at $x = 0, x = L$. The exterior problems are solved by the Laplace transformation

$$\hat{v}(x, s) = \int_0^\infty v(x, t) e^{-st} dt, \tag{3.18}$$

At the boundaries the following relations are obtained

$$\psi(L, t) = -\sqrt{\frac{\hbar}{2m\pi}} e^{i\frac{\pi}{4}} \int_0^t \frac{\psi_x(L, t - \tau) e^{-i\frac{V_L}{\hbar}\tau}}{\sqrt{\tau}} d\tau. \tag{3.19}$$

and

$$\psi(0, t) = -\sqrt{\frac{\hbar}{2m\pi}} e^{i\frac{\pi}{4}} \int_0^t \frac{\psi_x(0, \tau)}{\sqrt{t - \tau}} d\tau. \tag{3.20}$$

For numerical calculations, these continuous TBC should be discretized and used in connection with some appropriate numerical scheme for the PDE. Usually, the discretization schemes for the Schrödinger equation with TBC are based on the Crank - Nicolson finite difference scheme. But the discretization of such analytic TBC affects the unconditional stability of the Crank - Nicolson scheme and induces numerical reflections at the boundaries.

Ehrhardt and Arnold [20] proposed a discrete approach, in which the discretization of the PDE is considered first and then the TBC for the difference scheme is derived directly on a purely discrete level. This procedure prevents the numerical reflections due to additional

discretization errors at the boundary and inherits the unconditional stability of the whole-space Crank-Nicolson scheme.

In deducing the scheme, one make use of the discrete analogue of the Laplace transformation, the Z - transform:

$$\mathcal{Z}\{\psi_j^n\} = \hat{\psi}_j(z) := \sum_{n=0}^{\infty} \psi_j^n z^{-n}, \quad z \in \mathbf{C}, \quad |z| > 1. \quad (3.21)$$

The resulting *discrete* TBC at the grid point x_M reads

$$\psi_{M-1}^n - s^{(0)}\psi_M^n = \sum_{k=1}^{n-1} s^{(n-k)}\psi_M^k - \psi_{M-1}^{n-1}, \quad n \geq 1, \quad (3.22)$$

with

$$s^{(n)} = \left[1 - i\frac{R}{2} + \frac{\sigma}{2}\right] \delta_n^0 + \left[1 + i\frac{R}{2} + \frac{\sigma}{2}\right] \delta_n^1 + \alpha e^{-in\phi} \frac{P_n(\mu) - P_{n-2}(\mu)}{2n-1}, \quad (3.23)$$

$$R = \frac{4m(\Delta x)^2}{\hbar \Delta t}$$

$$\sigma = \frac{2m}{\hbar^2}(\Delta x)^2 V_L,$$

$$\phi = \text{arctg} \frac{2R(\sigma+2)}{R^2 - 4\sigma - \sigma^2},$$

$$\alpha = \frac{i}{2} \{(R^2 + \sigma^2) [R^2 + (\sigma+4)^2]\}^{1/4} e^{i\phi/2}.$$

$$\mu = \frac{R^2 + 4\sigma + \sigma^2}{\{(R^2 + \sigma^2)[R^2 + (\sigma+4)^2]\}^{1/2}},$$

P_n denotes the Legendre polynomials and δ_n^j the Kronecker symbol.

The coefficients $s^{(n)}$ can be calculated by the following recurrence relation:

$$s^{(n+1)} = \frac{2n-1}{n+1} \mu \lambda^{-1} s^{(n)} - \frac{n-2}{n+1} \lambda^{-2} s^{(n-1)}, \quad n \geq 2, \quad (3.24)$$

$$\lambda = \frac{R^2 - 4\sigma - \sigma^2 + 2iR(\sigma+2)}{\{(R^2 + \sigma^2)[R^2 + (\sigma+4)^2]\}^{1/2}},$$

the first values $s^{(n)}$ for $n = 0, 1, 2$ being obtained from eq. (3.23).

Note that in practice the condition $V(x) = V_L = \text{const.}$ for $x \geq L$, required by the method, is not always fulfilled, but if L is sufficiently large, $V(x)$ is varying very slowly for $x \geq L$ and one can take in calculations $V_L = V(L)$.

4 Applications

We used the above methods to compute proton decay rates for the ground state of spherical ^{109}I in two cases ($Q_p = 0.829$ MeV and $Q_p = 0.711$ MeV).

The potential used in TDSE was:

$$V(x) = V_n(x) + V_{so}(x) + V_c(x) + \frac{\hbar^2 l(l+1)}{2\mu x^2}$$

where

- V_n is the nuclear potential of Woods - Saxon form, i.e.

$$V_n = -\frac{D_n}{1 + \exp^{\frac{x-R_n}{a_0}}}$$

with D_n (the depth)= 61.3875 for the first case and 55.64 for the second case, R_n (the radius) = $r_0 A_2^{1/3}$, $r_0 = 1.17$, $A_2 = A - A_1$ ($A = 109$, $A_1 = 1$), a_0 (the diffuseness) = 0.75.

- V_{so} is the spin - orbit term and has the form

$$V_{so} = -\frac{D_{so} \times S \times \Lambda}{x \times a_{so}} \frac{\exp^{\frac{x-R_{so}}{a_{so}}}}{(1 + \exp^{\frac{x-R_{so}}{a_{so}}})^2}$$

with $D_{so} = 6.2$ and, respectively 5.61, S was taken equal to l , $\Lambda = 2$, $a_{so} = 0.75$, $R_{so} = r_{so} A_2^{1/3}$, $r_{so} = 1.01$.

- V_c is the coulombian potential, defined as

$$V_c = \begin{cases} \frac{Z_1 Z_2 e^2}{2R_c} [3 - (\frac{x}{R_c})^2], & x \leq R_c \\ \frac{Z_1 Z_2 e^2}{x}, & x > R_c. \end{cases}$$

with $Z_1 = 1$, $Z_2 = 52$, $R_c = r_c A_2^{1/3}$.

- the last term represents the centrifugal potential. We have taken $l = 2$ for the first energy and $l = 4$ for the second.

The initial wavefunction, i.e. the metastable state, was provided by solving the radial stationary Schrödinger equation in a modified potential (usually taking a constant value starting from some distance X_{mod} beyond the top of the barrier) with boundary conditions appropriate to bound states [$Q_p < V(X_{mod})$]. Actually, X_{mod} was equal to 50 fm and, respectively, 70 fm. These values should ensure a sufficiently large exponential decreasing tail of the wavefunction. In the figure 1 are shown the potentials (modified) with the first positive eigenenergies obtained in these potentials and the corresponding normalized eigenfunctions, used as initial wave functions in TDSE.

The success of the time - dependent approach to the decay of low - lying metastable states by quantum tunneling depends crucially on the preparation of this initial wave packet. In particular, it has to be as pure as possible to avoid the background produced by high energy components.

In TDSE is then used the original potential.

We have experimented the outlined methods of solution and artificial boundary conditions. We shall summarize below the results of tests.

The calculations were organized as follows.

The solution Φ of the stationary Schrödinger equation (with modified potential) is produced on some interval $[0, X_f]$. For TDSE this interval is extended to $[0, X_{max}]$ with $X_{max} = x_M = F \times X_f$. The initial wavefunction $\psi^I(x) = \Phi(x)$, $x \leq X_f$ and $\psi^I(x) = 0$, $x > X_f$. In the studied cases, $X_f = 128$.

The following physical quantities are calculated:

- a)- the norm of the wavefunction as a function of time,
- b)- the value of the energy during the propagation in time,
- c)- the quantity $\rho = Norm - Norm(int)$, where $Norm$ is the norm on the whole interval and $Norm(int)$ is the norm calculated between 0 and X_b , where X_b was chosen to be the last turning point ($X_b = 91.75$ and, respectively $X_b = 110.5$).

$\rho(t)$ represents the time dependent **Tunneling Probability**,

d)- the **decay rate** given by the relation:

$$\lambda(t) = \frac{1}{Norm - \rho(t)} \frac{d\rho(t)}{dt}. \quad (4.1)$$

In fact, in numerical calculations we found out that is more appropriate to determine ρ by $\rho = Norm(ext)$, where $Norm(ext)$ is the norm calculated in the limits X_b and X_{max} . We thus avoid the difference between two close quantities. Also, we replace $Norm - \rho(t)$ by $Norm(int)$. So that, we have used the following formula for the decay rate

$$\lambda(t) = \frac{1}{Norm(int)} \frac{d\rho(t)}{dt}. \quad (4.2)$$

Thus, double precision can still be used even for rather small decay rates.

Firstly, we have compared the three artificial boundary procedures implemented in Crank - Nicolson schemes in calculation of decay rates. We have used for the factor F the values 3, 4, 5. The spatial mesh size was $1/4$ and the time step $1/8$. The units are 'fm' and ' 10^{-22} sec'. The maximum time limit was of 300 units.

The figures 2, 3, 4 correspond respectively to TBC, ABC and DTBC for the first case ($E = 0.829$).

The three artificial boundary procedures have shown similar properties. They allow a reasonable size of the computational domain ($F = 5$) even for small decay rates, but the smoothness of the results deteriorates when further reducing the spatial grid ($F < 5$).

The TBC and DTBC procedures proved to be more convenient, since they adjust themselves the values of parameters involved, while ABC requires additional input parameters (the coefficients a_i). Actually we have taken all a_i equal for $p = 3$, depending on the parameter k_0 whose optimal value was found by tests. Thus $k_0 = 20$ and $a_1 = a_2 = a_3 = \frac{\hbar k_0}{m} = 4.3$. The DTBC requires a little extra computation and memory space in comparison with TBC.

In Fig.5 the result obtained with the same parameters on the interval $[0, 5 \times 128]$, but without TBC is given. One can see how the reflexions perturb the evolution of the solution and it is no longer possible to ascertain the asymptotic value.

We have found that without artificial boundary conditions a factor $F = 20$ would be necessary to avoid reflections.

Next, a MSD2 calculation is presented. To ensure the stability, a time step of $1/1024$ was necessary. We used TBC with a factor 5. The transparent boundary conditions are applied in the evaluation of the Hamiltonian (see eq. 2.16), namely the value Ψ_{M+1}^n is replaced by $\alpha \Psi_M^n$ where the coefficient α is obtained as explained before from the values of Ψ_M and Ψ_{M-1} at moment $n - 1$. In Fig. 6 it is shown the decay rate calculated in this way.

In the second case ($E = 0.711$) the results with the three artificial boundary conditions associated with Crank - Nicolson method are essentially similar to those obtained at $E = 0.829$. Only the asymptotic decay rate is smaller, namely with about 4 orders of magnitude smaller for a difference in energy of only 0.1 MeV.

In Fig. 7 the decay rate obtained with CN and TBC for $F = 5$ is presented.

MSD2 is less suited for this case. A smaller time step should be used to ensure stability, i.e. $1/2048$ and the TBC does not more work, due to the accumulation of the errors during the big amount of steps and the limits of the double precision used in calculations. Only a factor of 30 and no TBC have given reasonable result and it is shown in Figure 8.

Finally, we report the experiences with Chebyshev method. It allows a rather large time step ($1/8$ was used) but the number of terms in the sum giving the solution depends decisively on the magnitude of ΔE_{grid} . As this is related to V_{max} in such cases as considered, with singular potentials terms in origin, the maximum value of the potential on the grid is very large. Actually, it corresponds to $x = \Delta x$ and increases with l (the term $l(l+1)/x^2$ being

dominant near origin). We should take enough number (N_{bes}) of terms in the sum so that the Bessel coefficients decrease sufficiently and, therefore, the recurrence relation have to be used many times. This has consequence on the computing time and on the accumulated error. In our study cases, for $l = 2$ we got $\Delta E_{grid} = 5346$ and a number of $N_{bes} = 93$ was necessary to ensure a precision of 16 decimal digits, while for $l = 4$, $\Delta E_{grid} = 10056$ and $N_{bes} = 147$. Also, the Chebyshev method is not suitable for using the artificial boundary conditions, so that we needed an extension factor of 20 to avoid reflections. Figures 9 and 10 present Chebyshev calculations for the two cases considered.

The most convenient numerical method to solve the TDSE appeared to be Crank - Nicolson, with the modification proposed in the first section. The tridiagonal system solution at each time step is by far compensated by the step-size Δt admitted (much greater than for MSD2). Also, Crank Nicolson does not require time - consuming recurrence calculations as the Chebyshev scheme. Actually, a typical run with Crank Nicolson is of order of 30 seconds on a PC with AMD Athlon Processor at 1 GHz, while with the other methods the running time exceeds 1 hour.

Moreover, artificial boundary conditions (TBC, DTBC and ABC) can be easily incorporated into CN, thus reducing the length of the computational grid.

Since we considered the case of a spherical symmetry, the spatial coordinate in TDSE satisfies $x \geq 0$. The initial wave function has the value 0 in origin. The propagated solution is assumed to conserve this condition and therefore, the artificial BC's should be applied only on the right - hand boundary.

Let us note that the CN method, unconditionally conserving the norm and the energy, is best suited for such calculations, while the other methods require restrictive conditions to be satisfied for stability.

We add also a comparison with WKB approach. According to [21] the decay width is evaluated by

$$\Gamma = N \frac{\hbar^2}{4\mu} \exp\left\{-2 \int_{x_1}^{x_2} k(x) dx\right\}$$

where

$$k(x) = \sqrt{\frac{2\mu}{\hbar^2} |E - V(x)|}$$

$$N^{-1} = \frac{1}{2} \int_{x_0}^{x_1} \frac{dx}{k(x)}$$

and x_i , $i = 0, 1, 2$ are the classical turning points.

The decay rate is then

$$\lambda_{\infty} = \frac{\Gamma}{\hbar}.$$

Using the trapezoidal rule to evaluate the integrals we found the values :

1. for $E = 0.829$, $\lambda_{WKB} = 0.922 * 10^5 s^{-1}$, while $\lambda_{TDSE} = 0.786 * 10^5 s^{-1}$
2. for $E = 0.711$, $\lambda_{WKB} = 0.412 * 10^1 s^{-1}$, while $\lambda_{TDSE} = 0.322 * 10^1 s^{-1}$

The differences are not too large, but, of course, the WKB values are only approximations.

Let us also mention the estimates of half-life using TDSE. For $E = 0.829$ MeV, $t_{1/2} = \ln 2 / (0.786 * 10^5 s^{-1}) = 8.82 \mu s$, while for $E = 0.711$ MeV, $t_{1/2} = \ln 2 / (0.322 * 10^1 s^{-1}) = 0.215 s$.

5 Summary and Conclusions

The most intuitive and precise approach to the decay of a quasi - stationary state into the continuum is based on the solution of the time- dependent Schrödinger equation (TDSE). Numerically, this solution is always restricted to a finite portion of the infinite physical domain.

To avoid reflections from the numerical boundaries into the solution region, artificial boundary conditions have to be imposed. Moreover, if the energy of the quasi - stationary state is small compared to the top of the barrier (deep tunneling), the limit of the computing precision usually available is attained even for one - dimensional (in space) problems. The solution of TDSE can be found only using artificial BC's that efficiently reduce the reflections combined with a careful choice of the initial wave packet.

Three different artificial boundary conditions were implemented for the first time in the difficult case of deep tunneling: **transparent**, **absorbing** and **discrete transparent** boundary conditions.

The best results were obtained with the Crank - Nicolson method coupled with Transparent Boundary Conditions and very narrow initial wave packets. This allowed the length of the numerical grid to be reduced by a factor of 4 ($5 \times X_f$ instead of $20 \times X_f$).

The experience gained from this study is crucial for future studies of the more challenging case of multi - dimensional tunneling for long - lived metastable states. Also, the described procedures can be applied in other areas involving the solution of time-dependent Schrödinger equation, like chemical physics and laser physics.

References

- [1] O. Serot, N. Carjan, D. Strottman, *Transient behaviour in quantum tunneling: time - dependent approach to alpha decay*, Nucl. Phys. A **569** (3) (1994) 562 -574.
- [2] P. Talou, D. Strottman, N. Carjan, *Exact calculation of proton decay rates from excited states in spherical nuclei*, Phys. Rev. C **60** (5) (1999) 054318/1-7.
- [3] N. Carjan, P. Talou, M. Rizea, D. Strottman, *Proton emitting nuclei in a time - dependent formalism*, "Proton Emitting Nuclei", ed. J. Batchelder, AIP Conference Proceedings **518** (2000) 223 .
- [4] J. Crank, P. Nicolson, *A practical method for numerical evaluation of solutions of partial differential equations of the heat - conduction type*, Proc. Cambridge Philos. Soc. **43** (1947) 50 - 67.
- [5] W. H. Press, B. P. Flannery, S. A. Teukolsky, W. T. Vetterling, *Numerical Recipes*, Cambridge University Press (1989).
- [6] A. Askar, A. S. Cakmak, *Explicit integration method for the time - dependent Schrödinger equation for collision problems* , J. Chem. Phys. **68** (6) (1978) 2794 - 2798.
- [7] H. Tal-Ezer, R. Kosloff, *An accurate and efficient scheme for propagating the time-dependent Schrödinger equation*, J. Chem. Phys. **81** (9) (1984) 3967 - 3971.
- [8] J. M. Hymam, *Advances in Computer Methods for Partial Equations - III*, eds. R. Vichevetsky, R. Stepleman, IMACS, Bethlehem, PA (1979) 313.
- [9] C. Leforestier, R. H. Bisselinghe, C. Cerjan, M. D. Feit, R. Freisner, A. Guldberg, A. Hammerich, G. Jolicard, W. Karrlein, H. D. Meyer, N. Lipkin, O. Roncero and R. Kosloff, *A Comparison of Different Propagation Schemes for the Time Dependent Schrödinger Equation*, J. Comput. Phys. **94** (1991) 59 - 80.
- [10] T. Iitaka, *Solving the time - dependent Schrödinger equation numerically*, Phys. Rev. E **49** (5) (1994) 4684 - 4690.
- [11] G. Ronald Hadley, *Transparent boundary condition for beam propagation*, Optics Letters **16** (9) (1991) 624 - 626.
- [12] G. Ronald Hadley, *Transparent Boundary Condition for the Beam Propagation Method*, IEEE J. of Quantum Electronics **28** (1) (1992) 363 - 370.
- [13] T. Shibata, *Absorbing boundary conditions for the finite - difference time - domain calculation of the one - dimensional Schrödinger equation* , Phys. Rev. B **43** (1991) 6760 - 6763.
- [14] J. P. Kuska, *Absorbing boundary conditions for the Schrödinger equation on finite intervals*, Phys. Rev. B **46** (1992) 5000 - 5003.
- [15] T. Fevens and Hong Jiang, *Absorbing boundary conditions for the Schrödinger equation*, SIAM J. Sci. Comput. **21** (1) (1999) 255 - 282.
- [16] V. A. Baskakov and A. V. Popov, *Implementation of transparent boundaries for numerical solution of the Schrödinger equation*, Wave Motion **14** (1991) 123 - 128.

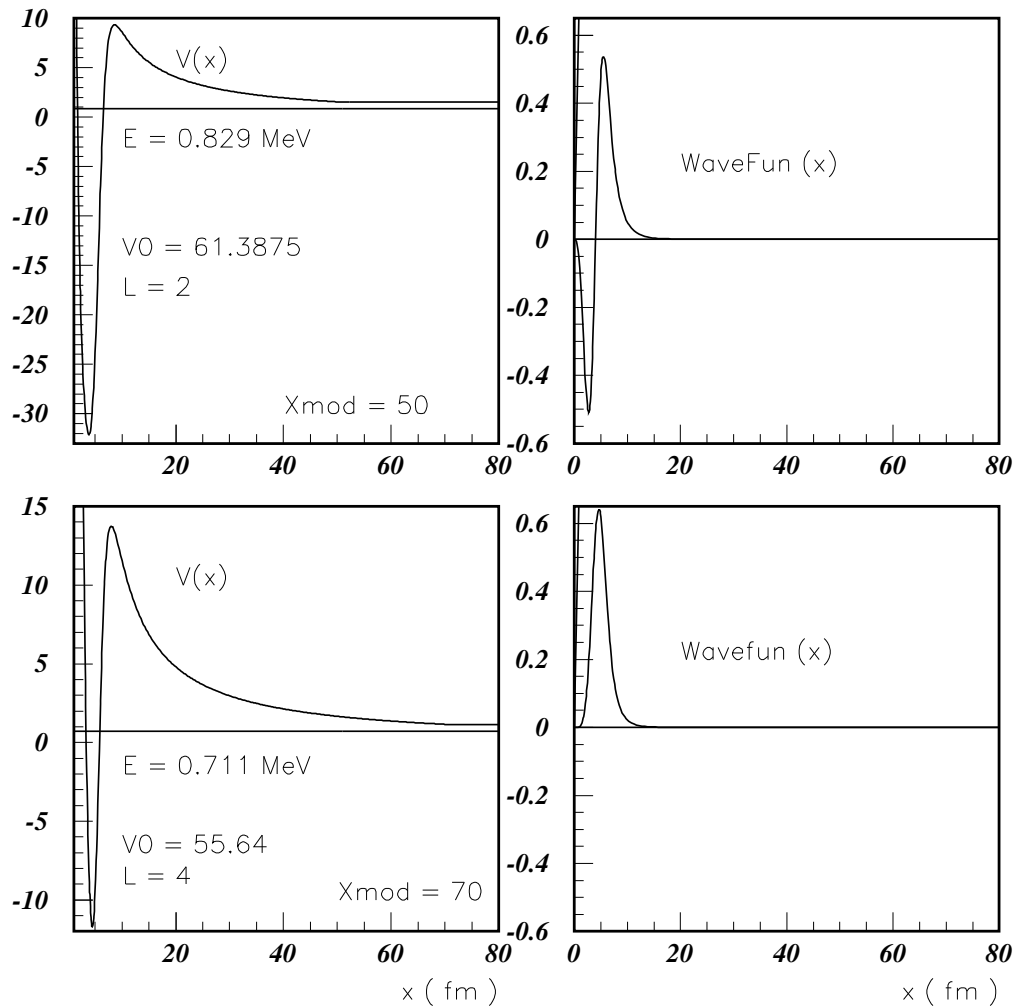


Figure 1: Eigenstates of the modified potentials used as initial states in TDSE

- [17] J. R. Hellums and W. R. Frensley, *Non-Markovian open-system boundary conditions for the time-dependent Schrödinger equation*, Phys. Rev. B **49** (1994) 2904 - 2906.
- [18] F. Schmidt and P. Deuffhard, *Discrete transparent boundary conditions for the numerical solution of Fresnel's equation*, Comput. Math. Appl. **29** (1995) 53 - 76.
- [19] F. Schmidt and D. Yevick, *Discrete transparent boundary conditions for Schrödinger-type equations*, J. Comput. Phys. **134** (1997) 96 - 107.
- [20] M. Ehrhardt and A. Arnold, *Discrete transparent boundary conditions for the Schrödinger equation*, Rev. di Matem. della Univ. di Parma **6/4** (2001) 57 - 108.
- [21] S. Aberg, P. Semmes, W. Nazarewicz, *Spherical proton emitters*, Phys. Rev. C **56/4** (1997) 1762 - 1773

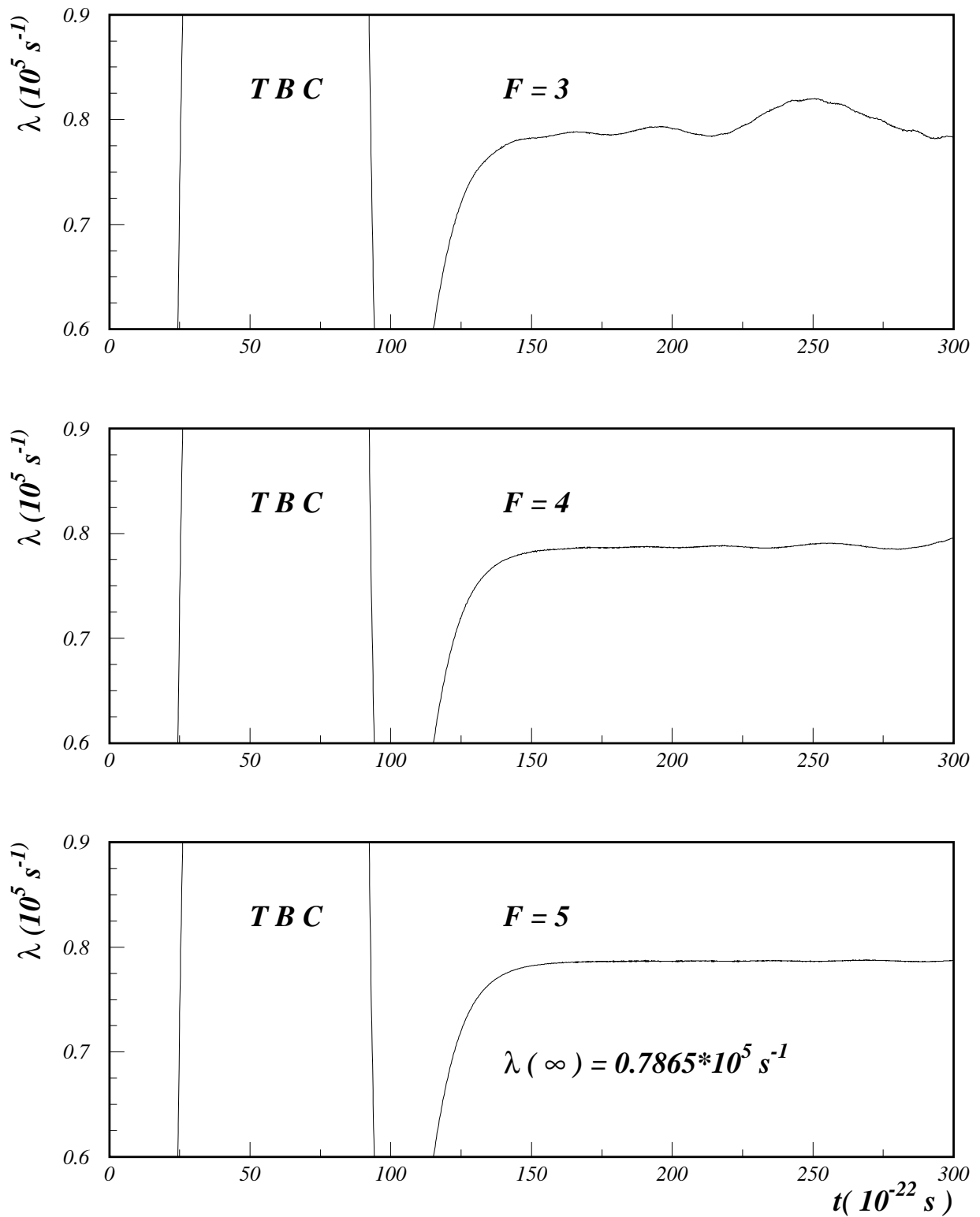


Figure 2: Decay rate calculated by integrating TDSE on a grid of total length $3, 4, 5 \times 128$ fm using Transparent Boundary Conditions implemented in Crank - Nicolson numerical scheme for $E=0.829$ MeV.

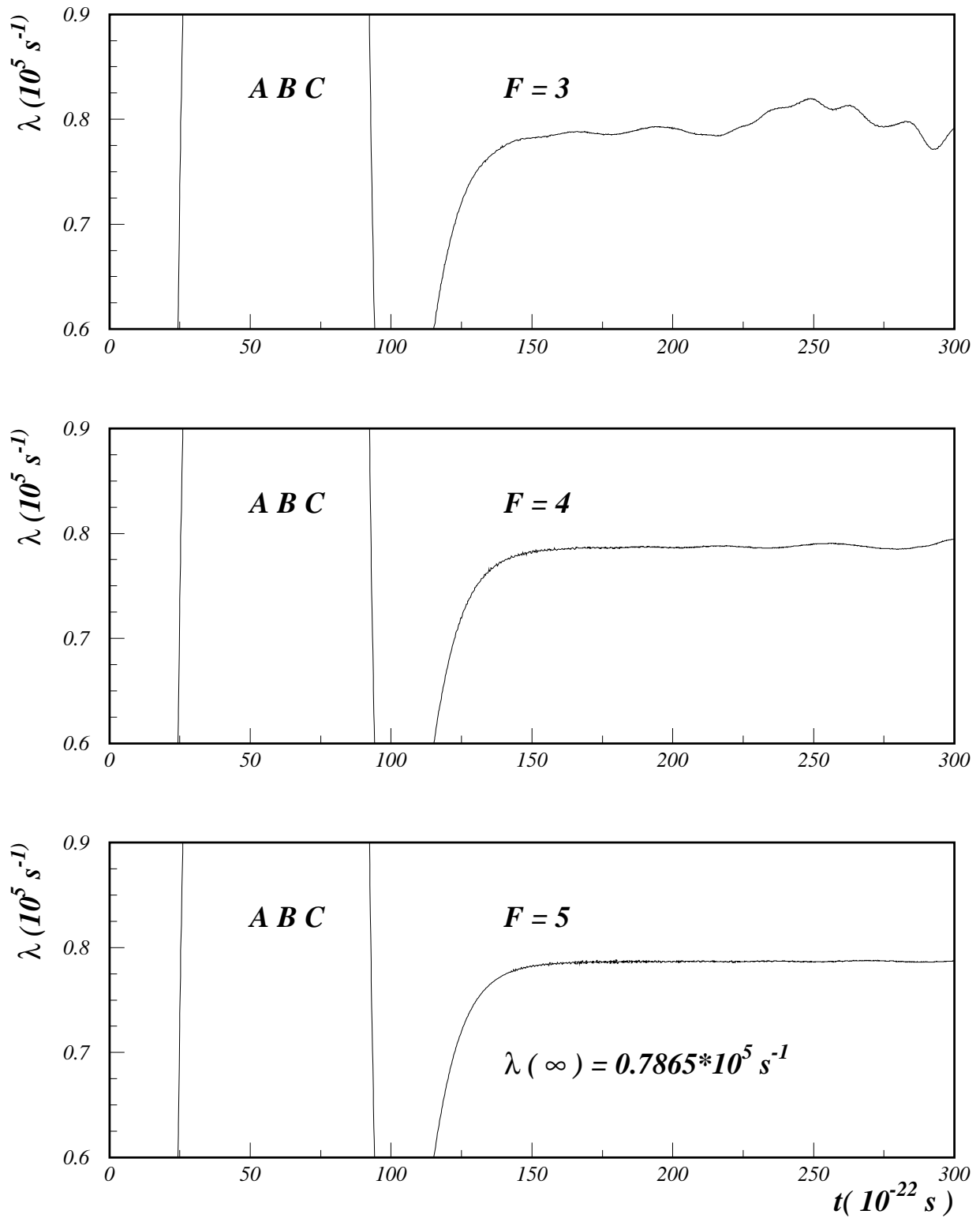


Figure 3: Same as in Fig. 2, using Absorbing Boundary Conditions of order $p = 3$.

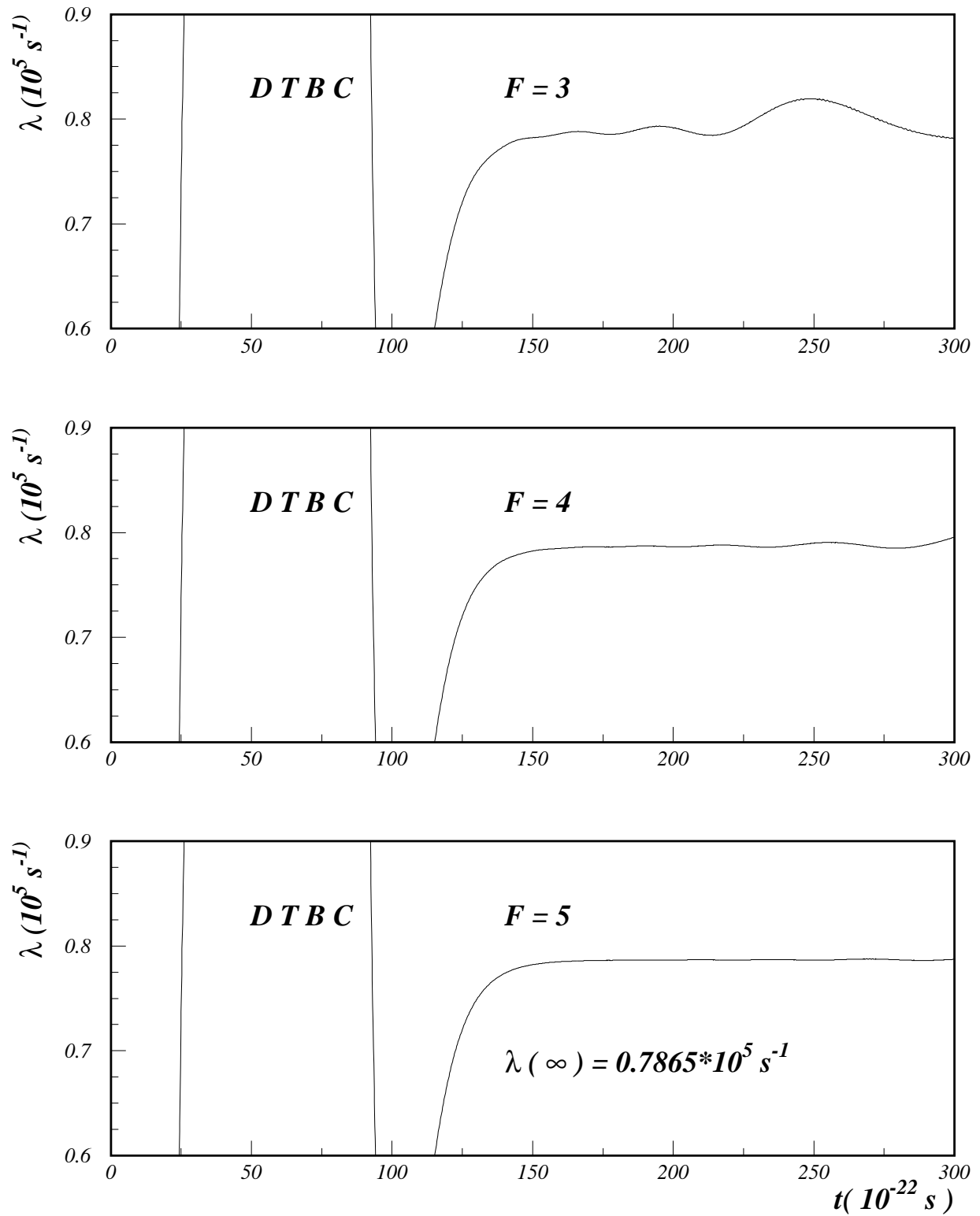


Figure 4: Same as in Fig. 2 with Discrete Transparent Boundary Conditions.

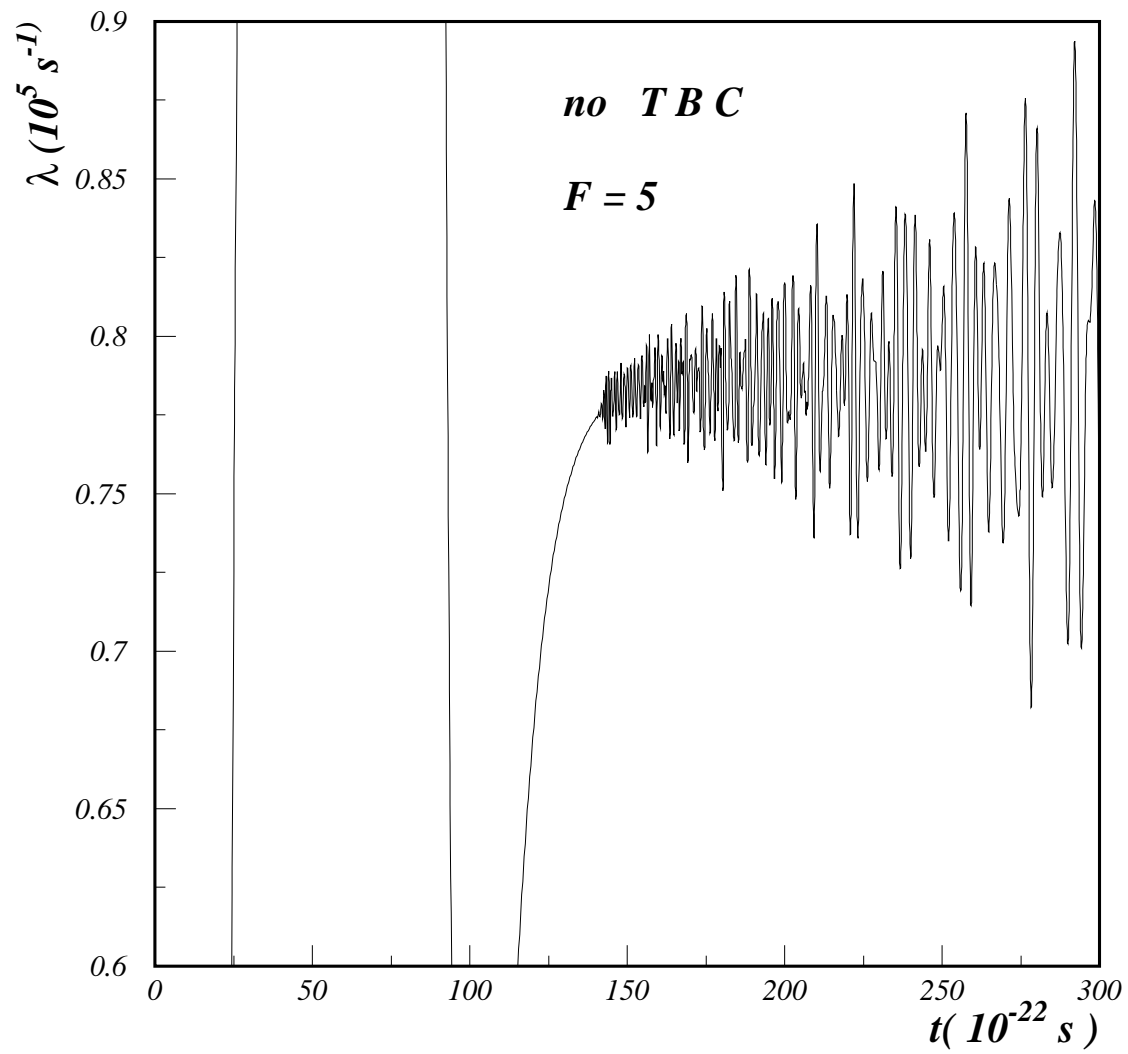


Figure 5: Decay rate using a grid of length 5×128 but without implementing TBC.

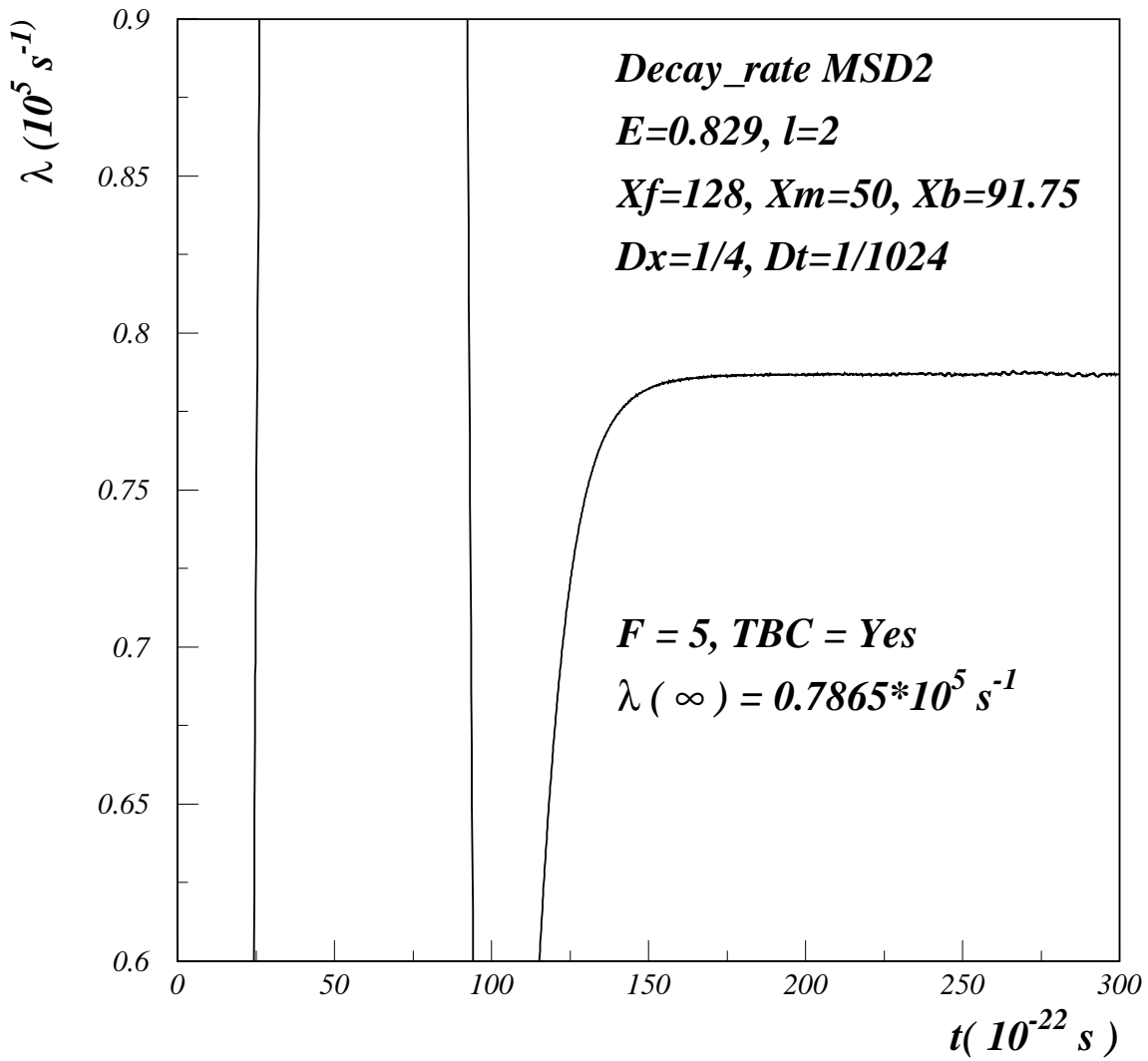


Figure 6: Decay rate calculated by integrating TDSE using MSD2 numerical scheme at $E = 0.829$ MeV

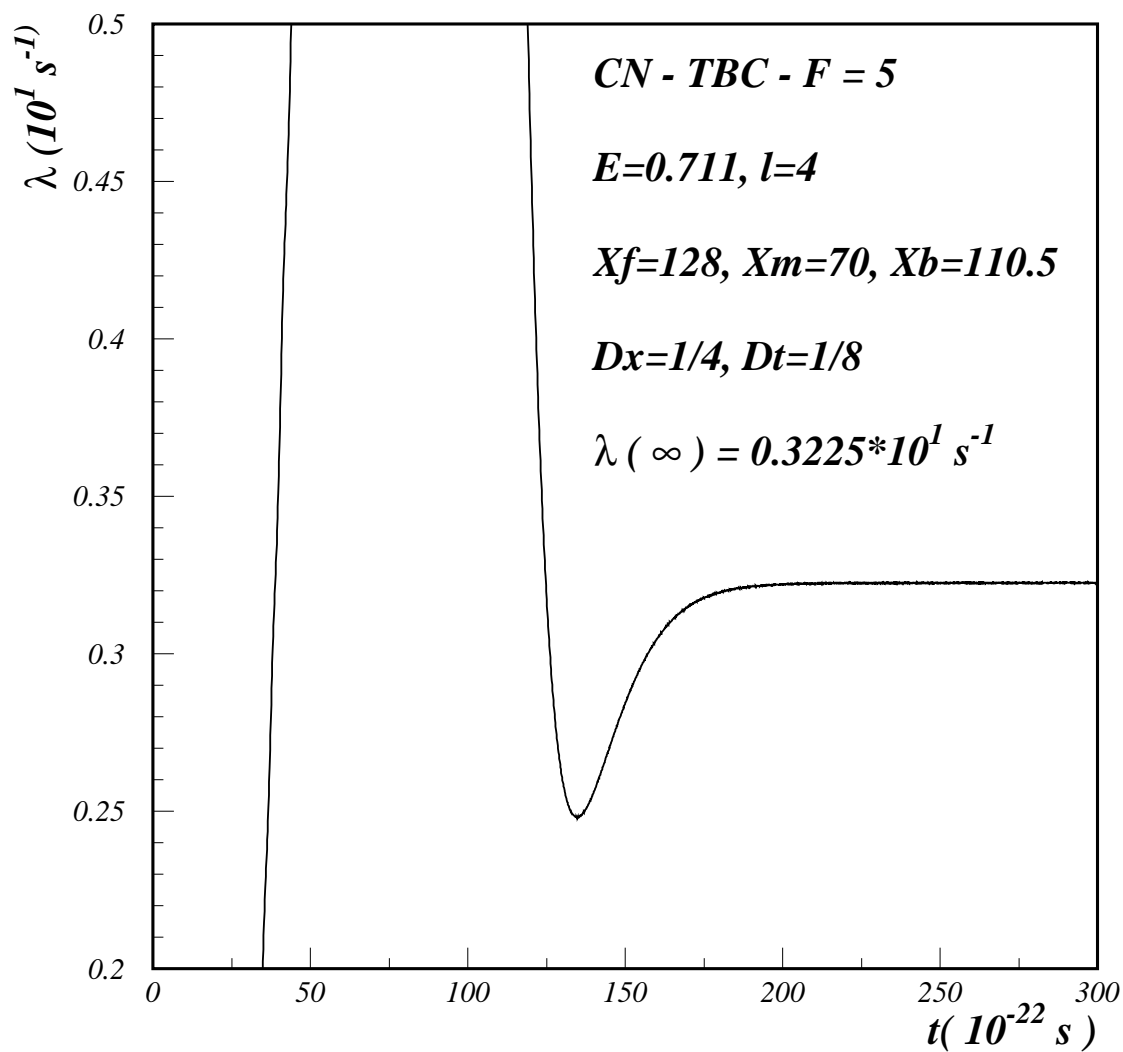


Figure 7: Decay rate calculated by integrating TDSE on a grid of total length 5×128 fm using Transparent Boundary Conditions implemented in Crank - Nicolson numerical scheme for $E = 0.711$ MeV

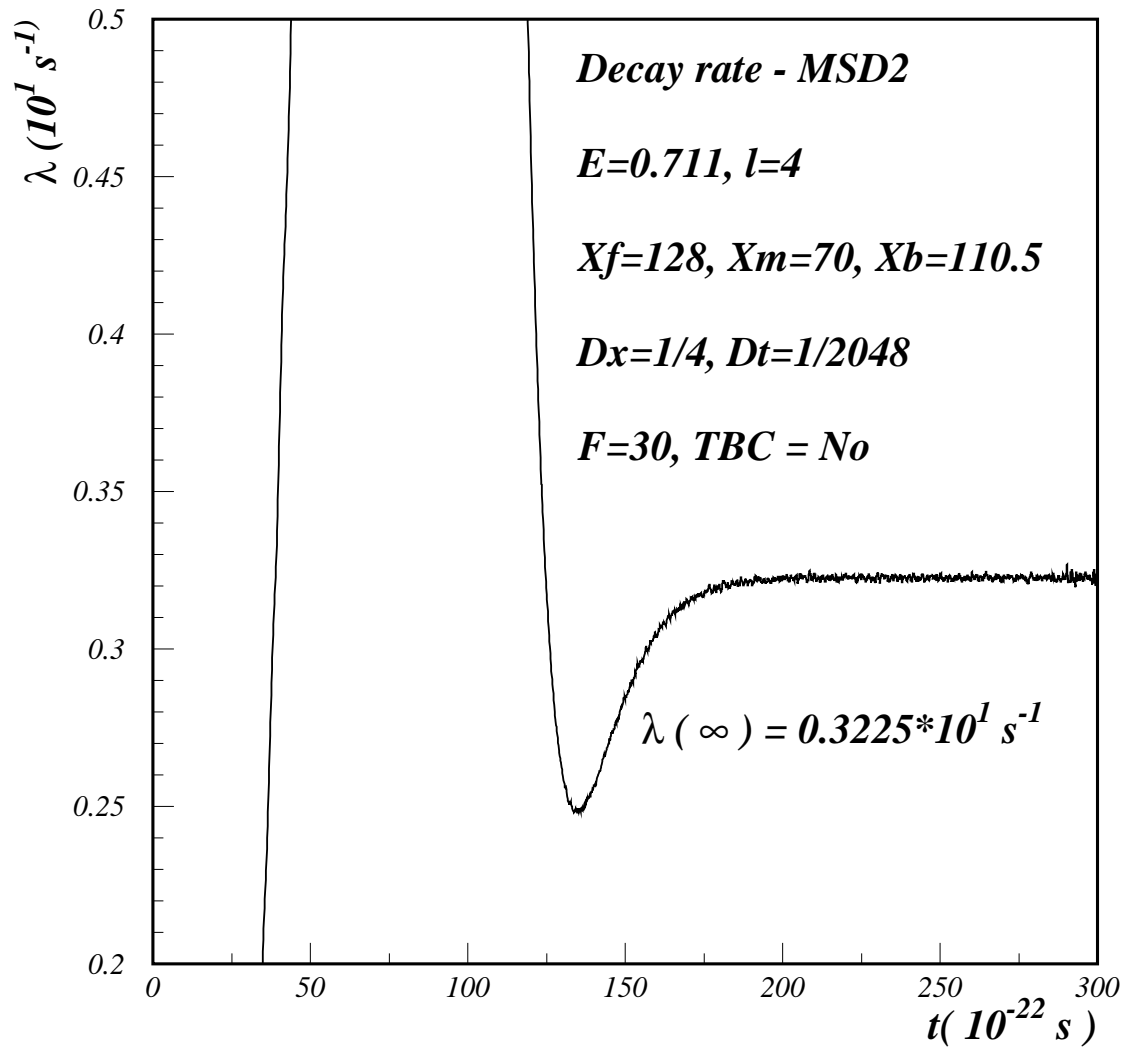


Figure 8: Decay rate calculated by integrating TDSE using MSD2 numerical scheme at $E = 0.711$ MeV

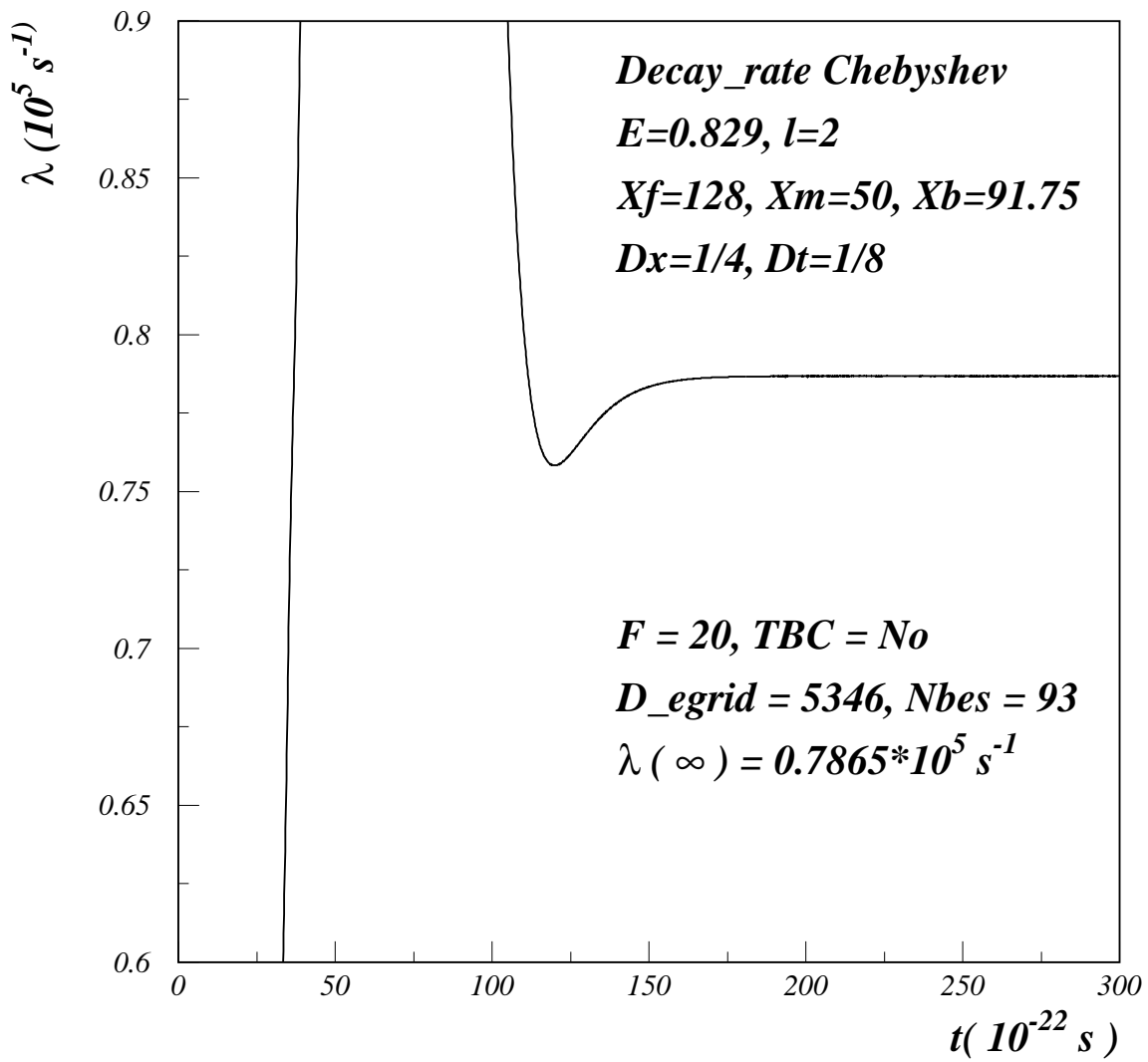


Figure 9: Decay rate calculated by integrating TDSE using Chebyshev numerical scheme at $E = 0.829$ MeV

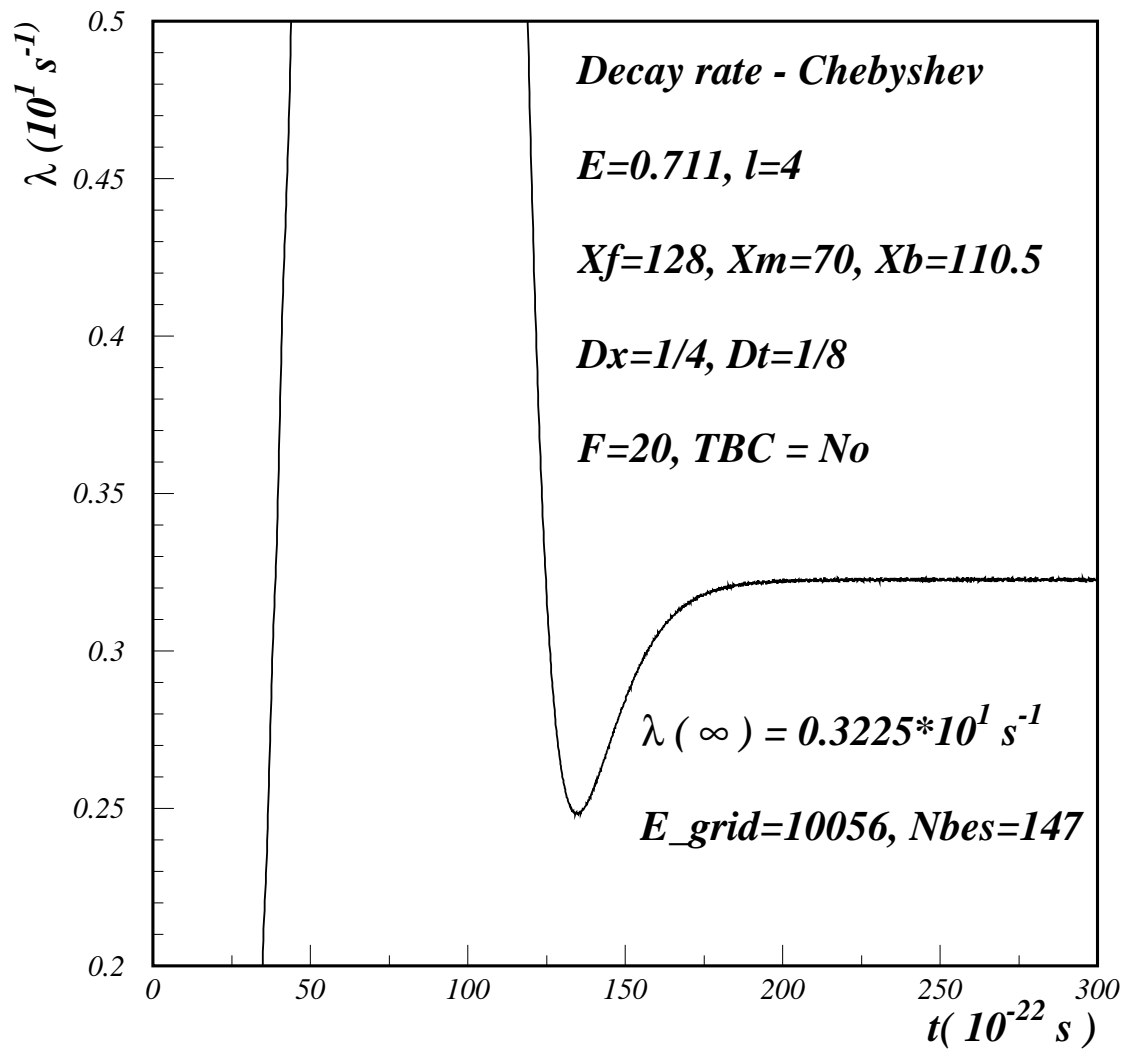


Figure 10: Decay rate calculated by integrating TDSE using Chebyshev numerical scheme at $E = 0.711$ MeV